SEASONAL DYNAMICS OF GEOMAGNETIC STORMS

Bishir Usman[1], Ibrahim Jafaru[2]

[1]Department of Basic and Applied Science, Hassan Usman Katsina Polytechnic, Katsina, Katsina State, Nigeria, email:
[2]Department of Physics, Isa Kaita College of Education, Katsina, Katsina State, Nigeria

***Abstract*: This study is based on the seasonal dynamic of geomagnetic storms. The 1 hour Dst geomagnetic index was used in this work to characterize the geomagnetic storm development and it was obtained from the World Data Centre for Geomagnetism, WDC-Kyoto. One-hour data of the vertical component of interplanetary magnetic field IMF-z and solar wind ion parameters; proton density (Np), proton temperature (Tp) and proton speed (Vp) were obtained from the MAG and SWEPAM experiments on the Advance Composition Explorer (ACE) spacecraft, as given by the ACE Science Centre. The period selected for the analysis is the ACE observational period from 2011 to 2018, for which the Dst index was available in its final form when this work was performed. Intense geomagnetic storms that reaches, at least, a Dst peak of −100 nT were selected. Considering this criterion, a total of 20 events were obtained. From this data-set, 8 storms were used in the study, out of which three are selected each from summer and equinox and two from winter. Base on the analysis of the data it is observed that disturbed storm index (Dst) lags behind vertical component of interplanetary magnetic field IMF-z with a range of 3-11UTC in summer season, 1-6UTC in winter and 6-14UTC in equinox. This means that the time delay between vertical component of interplanetary magnetic field and disturbed storm index is comparably highest in equinox and least in winter.**

***Keywords*: seasonal variation, geomagnetic storm, solar proton density, solar proton temperature, solar proton speed, interplanetary magnetic field and disturbed storm index.**

INTRODUCTION

The fluctuations in the solar magnetic field is transported via the solar wind to the interplanetary space which distorts the earths roughly dipolar magnetic field to a complex form called the magnetosphere. The magnetosphere is home to several current systems, the ring current of which produces a magnetic field that is diametrically opposed to the earth's magnetic field, and thus fluctuations in the former affect the latter. A storm occurred when the resultant horizontal component of the geomagnetic field reaches a value of -50nT. Fluctuation in geomagnetic activity or geomagnetic storms is a nuisance to ionospheric propagation. Thus prediction about the occurrence and strength of a geomagnetic storm constitutes a very important part of space physics [1]. Since several decades, it has been known that geomagnetic activity is higher on average at the equinoxes than at the solstices. Only recently, it has been noticed that this seasonal variation is especially prominent when large geomagnetic storms are considered [2]. However, there is currently no accepted explanation for this behaviour of great storms. Geomagnetic storms are significant perturbations of the geomagnetic field from normal behaviour, analogous to weather storms on Earth's surface. Geomagnetic storms represent the single most important space weather phenomenon and also are an exciting and rewarding topic that covers an interesting spectrum of ionosphere-magnetosphere interactions [3]. Geomagnetic storms are caused mainly by solar wind transients from the coronal mass ejections (CMEs) and solar flares or by the corotating interaction regions (CIRs) formed during the interaction between the high and low speed streams. Occurrence frequency and intensity of transient solar emissions vary with different phases of the solar cycle characterized by the number of sunspots on the photosphere. Solar maximum is dominated by powerful solar eruptions, like solar flares and CMEs. On the other hand, the solar minimum is featured by coronal holes and fast wind streams [4]. Most dominant mechanism for transfer of solar wind energy into the magnetosphere to produce the geomagnetic storms is magnetic reconnection between southwardly oriented IMF Bz component and the antiparallel geomagnetic field lines. These geomagnetic storms in the Earth's magnetosphere and ionosphere subsequently intense auroral activity, satellite damage, transformer failures and tripping of power grids.

SEASONAL VARIATION

Seasonal variation is variation in a time series within one year that is repeated more or less regularly. Seasonal variation may be caused by the temperature changes. Astronomical seasons are based on the position of the Earth in relation to the sun, whereas meteorological seasons are based on the annual temperature cycle. The Earth's annual trip around the sun forms the basis for the astronomical calendar in which seasons are defined by two solstices and two equinoxes. The Earth is tilted 23.5 degrees on its axis of rotation, and how the North Pole is oriented toward or away from the sun determines two of these astronomical dates [5]. At the winter solstice, the North Pole is tilted away from the sun, whereas at the summer solstice, the North Pole is tilted toward the sun. The equinoxes occur halfway between these events when the sun's path is aligned with the Earth's equator. Meteorological seasons are broken down into groupings of three months in our civil calendar based on the annual temperature cycle. We generally think of winter as the coldest time of the year and summer as the warmest time of the year, with spring and fall being the transition seasons. In the Southern Hemisphere, the seasons are reversed where summer occurs when the South Pole is oriented towards the sun, and winter happens when the South Pole faces away. The Northern Hemisphere experiences more direct sunlight during May, June, and July, as the hemisphere faces the Sun. The same is true of the Southern Hemisphere in November, December, and January. It is Earth's axial tilt that causes the Sun to be higher in the sky during the summer months, which increases the solar flux. [6] However,

due to seasonal lag, June, July, and August are the warmest months in the Northern Hemisphere while December, January, and February are the warmest months in the Southern Hemisphere. The following table shows the seasonal classification in Northern and Southern Hemisphere

Table 1 Seasonal Variations in Northern and southern Hemisphere

	Winter	Summer	Equinox
Northern Hemisphere	January, February, November, December	May, June, July, August	March, April, September, October
Southern Hemisphere	May, June, July, August	January, February, November, December	March, April, September, October

GEOMAGNETIC STORM:

A geomagnetic storm is defined by changes in the Dst (disturbance – storm time) index. The Dst index estimates the globally averaged change of the horizontal component of the Earth's magnetic field at the magnetic equator based on measurements from a few magnetometer stations. Dst is computed once per hour and reported in near-real-time. During quiet times, Dst is between +20 and −20 nano-Tesla (nT) [7].

Table 2: Phases of Geomagnetic Storms:

A geomagnetic storm has three phases: initial, main and recovery.

INITIAL PHASE	MAIN PHASE	RECOVERY PHASE
The initial phase is characterized by Dst (or its one-minute component SYM-H) increasing by 20 to 50 nT in tens of minutes. The initial phase is also referred to as a storm sudden commencement (SSC).	The main phase of a geomagnetic storm is defined by Dst decreasing to less than −50 nT. The selection of −50 nT to define a storm is somewhat arbitrary. The duration of the main phase is typically 2–8 hours.	The recovery phase is when Dst changes from its minimum value to its quiet time value. The recovery phase may last as short as 8 hours or as long as 7 days.

Table 3: Classification of Geomagnetic Storms on the Basis of Intensity:

MODERATE	INTENSE	SUPER STORM
−50 nT > minimum of Dst >−100 nT	−100 nT > minimum Dst > −250 nT)	Minimum of Dst < −250 nT

During geomagnetic storms the magnetic field in the magnetosphere and on the ground is strongly disturbed globally. The perturbation of the magnetic field during a storm is due the enhancement of the equatorial ring current. This constant but time dependent westward current consisting mainly of the westward drift of positively charged particles but also the eastward drift of negatively charged particles. During storm time the ring current is enhanced and moved spatially closer to the ground. This causes a disturbance in the H compound of the magnetic field. It can be detected on the ground, as indeed done at the multiple magnetic observatories. The storms are classified according to some criteria, most often a specific index calculated from the magnetic measurements of subset of the observatories. Being global events, the disturbance of the magnetic field during magnetic storms has to be detected by several stations at once to qualify. The most common index to satisfy the magnitude of the storm is the Dst index. Since no magnetic storm is quite the same due to their complicated origins and dynamics the statistical approach used here has to be used with care. [8]

METHEDOLOGY:

This study is based on the seasonal dynamics of geomagnetic storms. The 1 hour Dst geomagnetic index was used in this work to characterize the geomagnetic storm development and it was obtained from the World Data Centre for Geomagnetism, WDC-Kyoto. One-hour data of the vertical component of interplanetary magnetic field IMF-z and solar wind ion parameters; proton density (Np), proton temperature (Tp) and proton speed (Vp) were obtained from the MAG and SWEPAM experiments on the Advance Composition Explorer (ACE) spacecraft, as given by the ACE Science Centre. The period selected for the analysis is the ACE observational period from 2011 to 2018, for which the Dst index was available in its final form when this work was performed. Intense geomagnetic storms that reached, at least, Dst peak of −100nT were selected. Considering this criterion, a total of 20 events were obtained. The events were classified into Summer Geomagnetic Storms (consisting of events that occur in May, June, July and August), Winter Geomagnetic Storms (consisting of events that took place in January, February, November and December) and Equinox Geomagnetic Storms (consisting of events that occur in March, April, September and October). Six events were obtained in summer out of which three were selected, four events were obtained in winter out of which two were selected and in equinox three events were chosen out of ten events obtained.

OBSERVATIONS TABLES

TABLE 4: Summer Geomagnetic Storm

SERIAL No.	YEAR	MONTH	DATE	Dst Index	Dst Time (UTC)	Max. N_p (cm^{-3})			Max. T_p (°K)			Max. V_p (km/s)			Max. IMF-z (nT)		
						N_p (cm^{-3})	Date	time	T_p (°K)	date	Time (UTC)	V_p (km/s)	date	Time	IMF-z (nT)	date	time
1	2011	AUGUST	6	-115	4:00	46.95	5	19	6.26E+05	5	22	672.6	5	22	-21.17	5	20
2	2012	JULY	15	-139	19:00	39.81	15	5	6.45E+05	14	18	701.71	14	23	-19.81	15	8
3	2013	JUNE	1	-124	9:00	36.50	31	23	6.22E+05	1	23	810.46	2	15	-21.21	1	0
4	2015	JUNE	23	-204	5:00	59.43	22	18	8.47E+05	24	17	808.31	23	6	-39.44	22	18
5	2017	MAY	28	-125	8:00	59.36	27	19	2.88E+05	29	15	429.17	29	15	-20.20	28	0
6	2018	AUGUST	26	-175	7:00	27.62	26	12	3.13E+05	27	18	643.23	27	18	-17.04	26	4

TABLE 5: Winter Geomagnetic Storm

SERIAL No.	YEAR	MONTH	DATE	Dst Index (nT)	Dst Time (UTC)	Max. N_p (cm^{-3})			Max. T_p (°K)			Max. V_p (km/s)			Max. IMF-z (nT)		
						N_p (cm^{-3})	date	Time (UTC)	T_p (°K)	date	Time (UTC)	V_p (km/s)	date	Time (UTC)	IMF-z (nT)	Date	Time (UTC)
1	2012	NOVEMBER	14	-108	8	26.22	14	4	3.13E+05	13	1	495.02	13	1	-19.12	14	2
2	2014	FEBRUARY	19	-119	9	24.56	19	9	5.33E+05	20	2	741.16	20	4	-15.40	19	3
3	2015	DECEMBER	20	-155	23	38.45	20	12	2.60E+05	19	16	502.04	19	20	-18.91	20	22
4	2016	JANUARY	1	-110	1	30.66	31	13	3.49E+05	31	4	501.07	31	8	-16.30	31	19

TABLE 6: Equinox Geomagnetic Storm

SERIAL No.	YEAR	MONTH	DATE	Dst Index (nT)	Dst Time (UTC)	Max. N_p (cm^{-3})			Max. T_p (°K)			Max. V_p (km/s)			Max.IMF-z (nT)		
						N_p(cm^{-3})	date	Time (UTC)	T_p(°K)	date	Time (UTC)	V_p(km/s)	date	Time (UTC)	IMF-z (nT)	date	Time (UTC)
1	2011	SEPTEMBER	26	-118	24	16.47	25	16	6.68E+05	26	21	698.48	26	23	-31.01	26	13
2	2011	OCTOBER	25	-147	2	No data	No data	No data	4.17E+05	24	18	564.65	25	0	-20.37	24	20
3	2012	MARCH	9	-145	9	5.18	10	21	1.50E+05	10	3	641.17	9	16	-18.27	9	3
4	2012	APRIL	24	-120	5	No data	No data	No data	6.45E+05	25	18	772.22	25	18	-15.58	23	17
5	2012	OCTOBER	1	-122	5	No data	No data	No data	1.52E+05	1	15	428.62	1	0	-20.80	1	0
6	2013	MARCH	17	-132	21	26.15	17	7	6.44E+05	17	5	761.64	17	10	-19.07	17	7
7	2015	MARCH	17	-222	23	33.52	17	4	6.17E+05	17	11	737.92	18	21	-28.56	17	13
8	2015	OCTOBER	7	-124	23	28.68	7	12	6.82E+05	7	19	840.94	7	20	-18.41	7	13
9	2016	OCTOBER	13	-104	24	23.00	13	2	2.27E+05	14	23	445.77	14	15	-21.17	13	15
10	2017	SEPTEMBER	8	-122	2	15.89	7	6	1.24E+06	8	1	855.47	8	7	-31.62	7	23

RESULTS

From the study it is clearly observed that disturbed storm index (Dst) lags behind vertical component of interplanetary magnetic field (IMF-z) with a range of 3-11UTC in summer season, 1-6UTC in winter and 6-14UTC in equinox. This means that the time delay between vertical component of interplanetary magnetic field and disturbed storm index is comparably highest in equinox and least in winter. Thus the result obtained in this research shows clearly that the delay time between vertical interplanetary magnetic field and disturbed storm index can be used to predict the time interval between vertical interplanetary magnetic field and occurrence of storm, so that drastic measures can be taken to avert or minimize its negative effects.

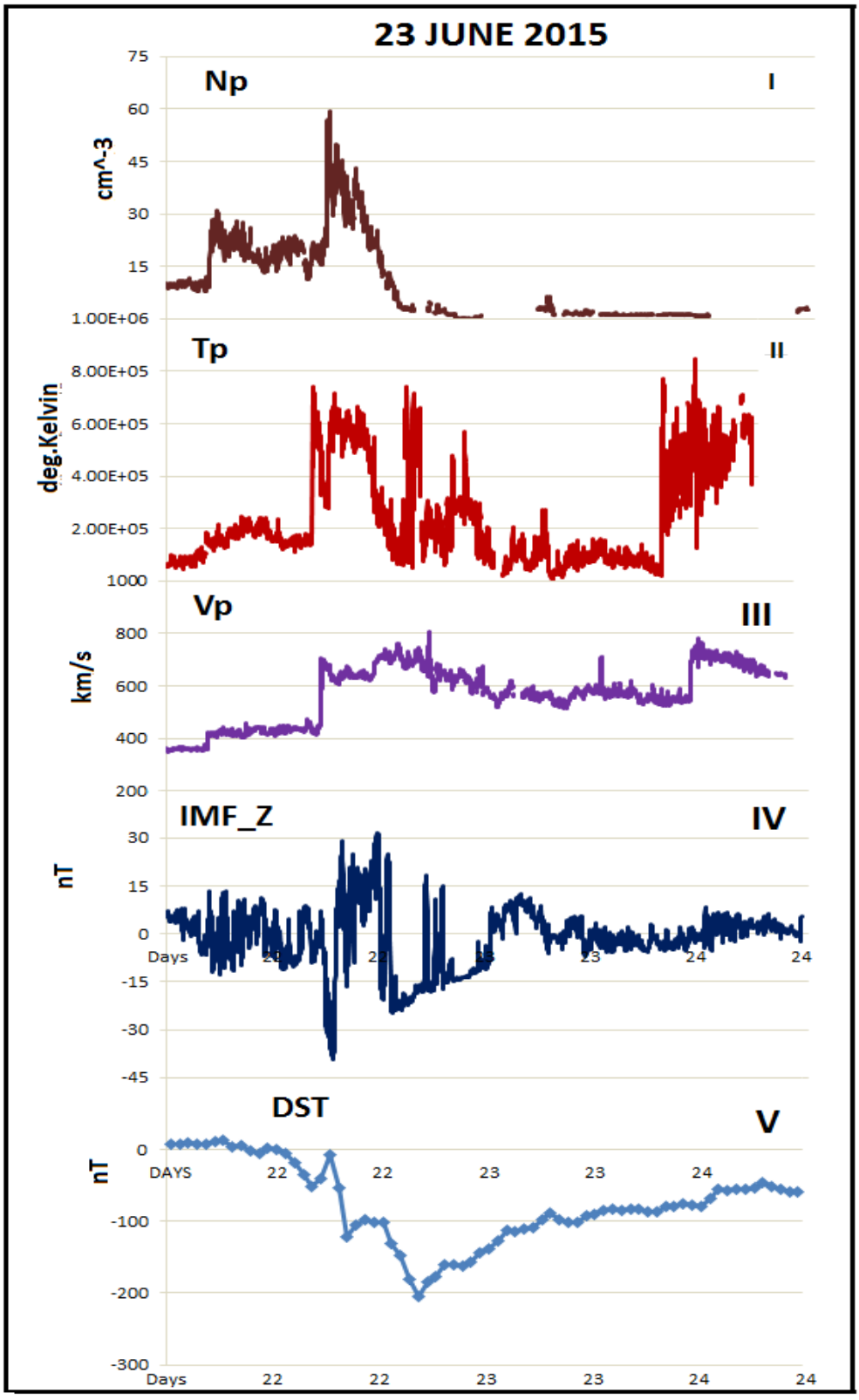

Figure 1: There are five panels in the figure. 1st, 2nd and 3rd panels are solar wind proton density in cm^{-3}, proton temperature in °K and proton speed in km/s respectively, 4th and 5th panels are Dst index and vertical component of IMF both measured in nT.

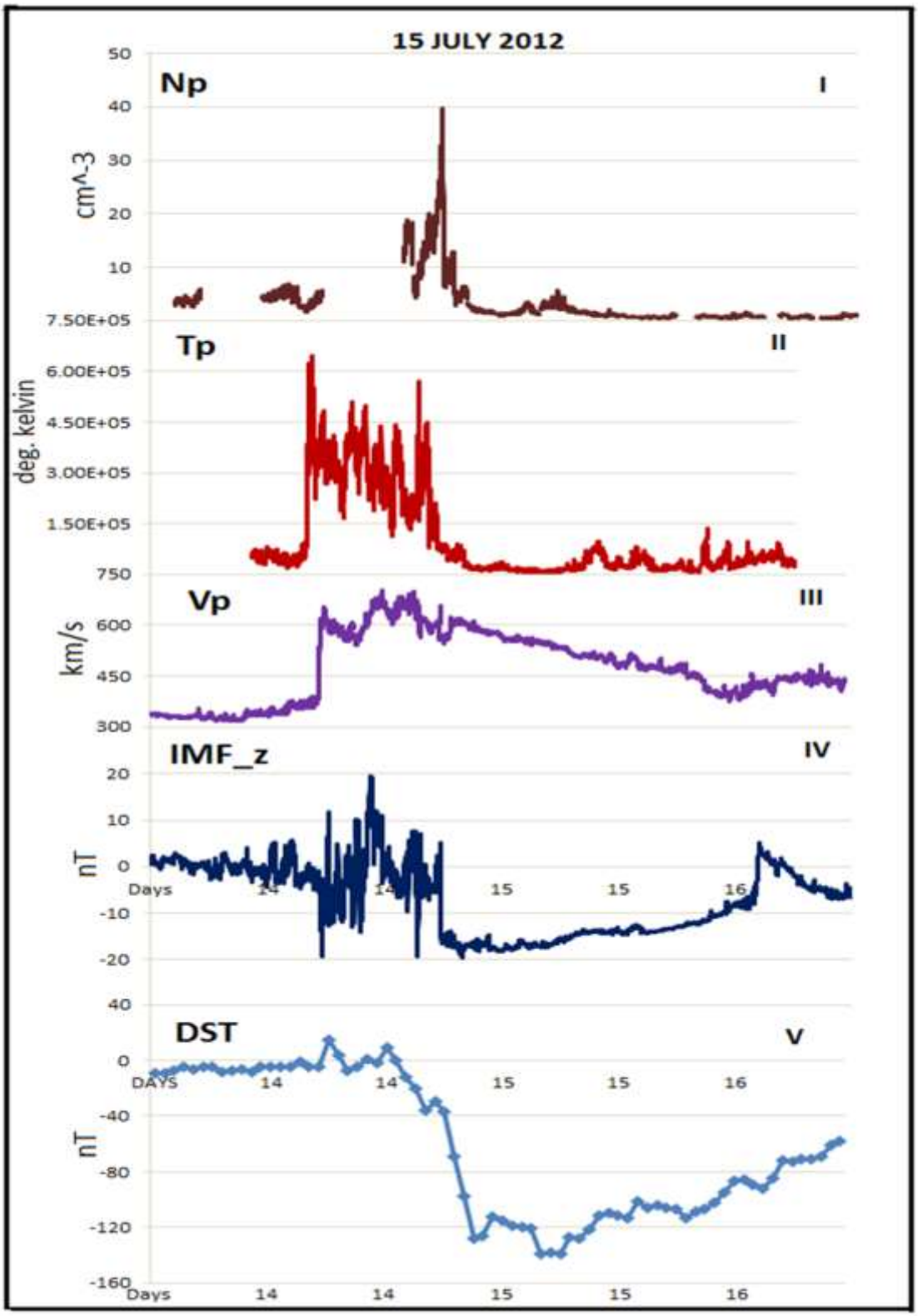

Figure 2: There are five panels in the figure. 1st, 2nd and 3rd panels are solar wind proton density in cm^{-3}, proton temperature in °K and proton speed in km/s respectively, 4th and 5th panels are Dst index and vertical component of IMF both measured in nT.

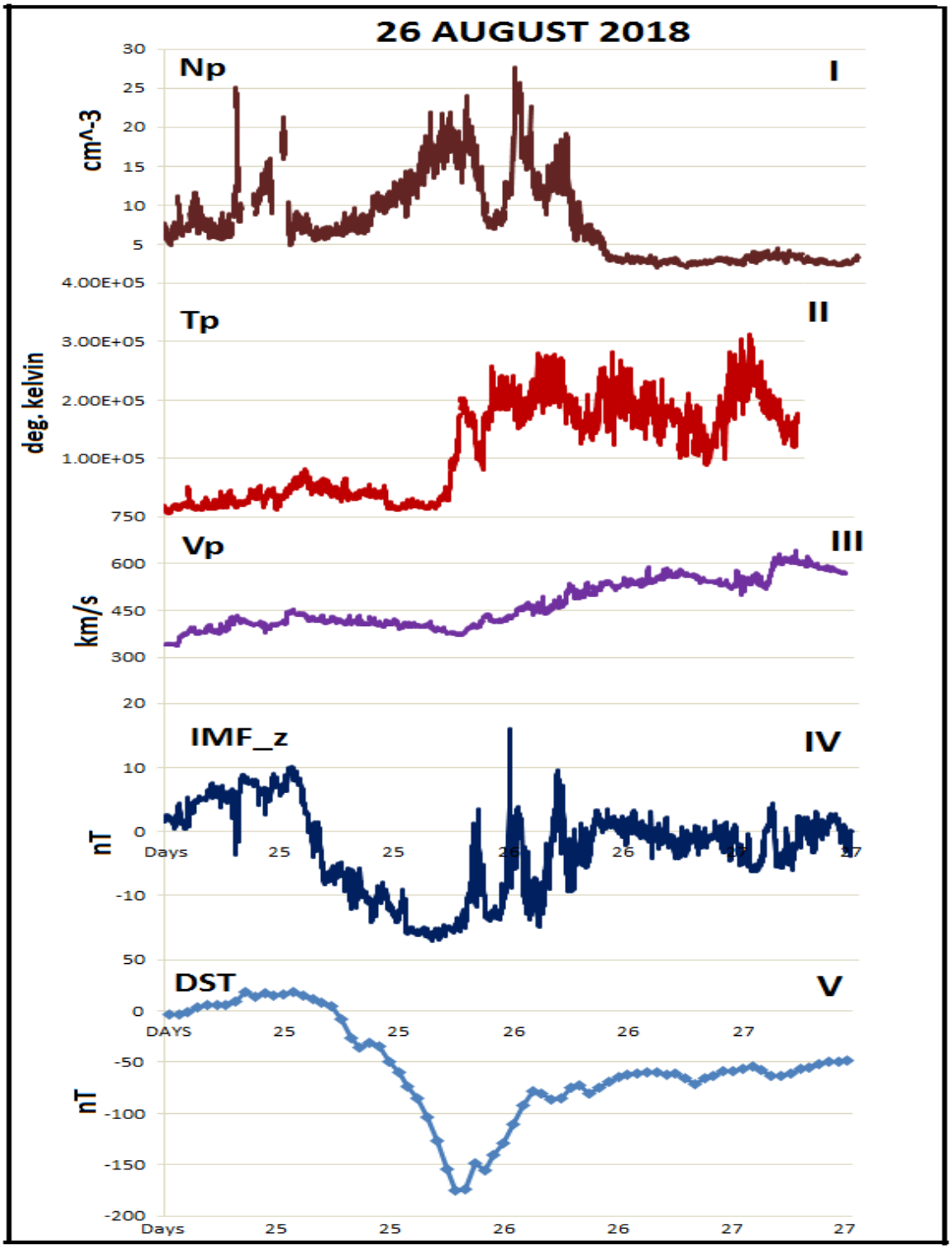

Figure 3: There are five panels in the figure. 1st, 2nd and 3rd panels are solar wind proton density in cm^{-3}, proton temperature in °K and proton speed in km/s respectively, 4th and 5th panels are Dst index and vertical component of IMF both measured in nT.

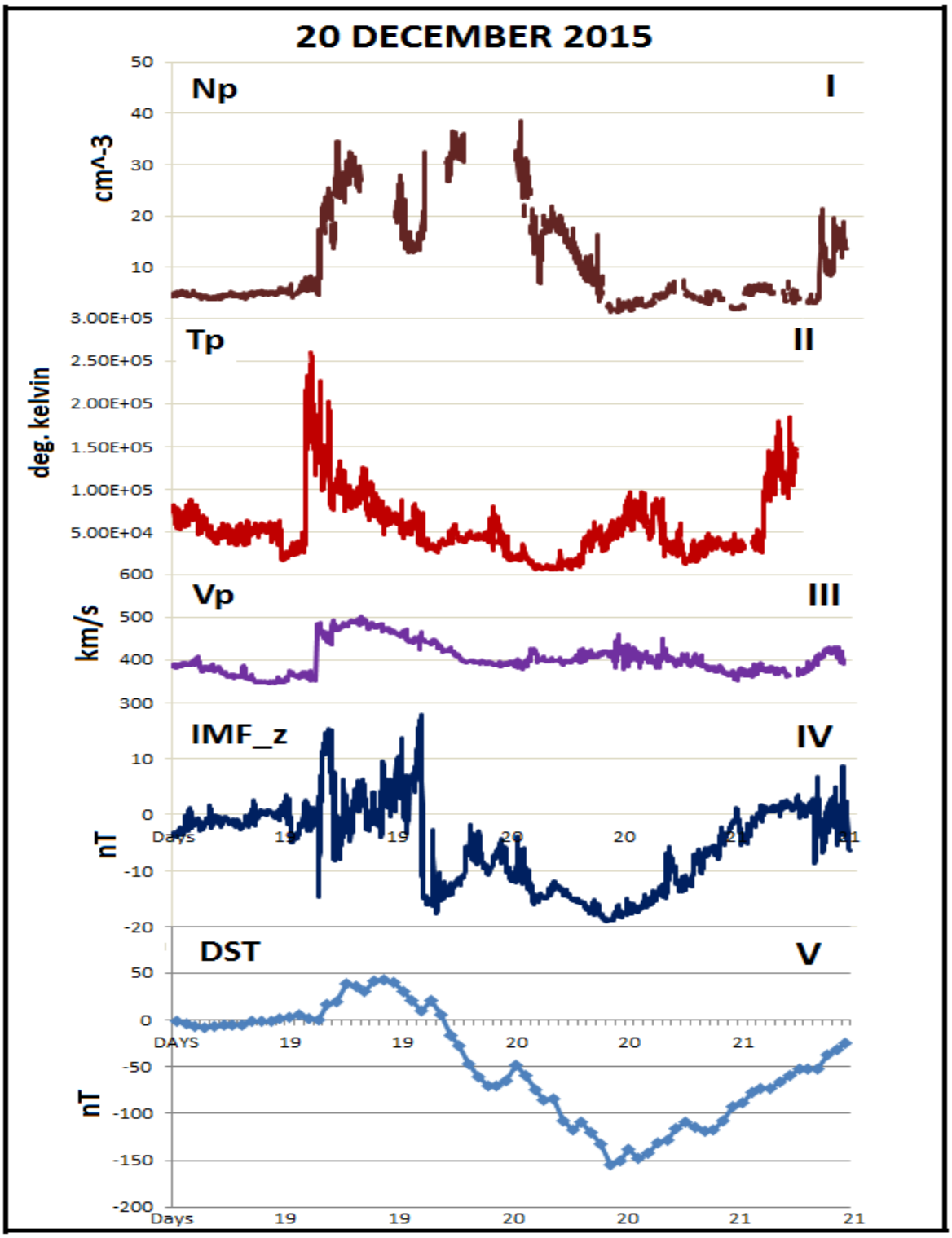

Figure 4: There are five panels in the figure. 1st, 2nd and 3rd panels are solar wind proton density in cm^{-3}, proton temperature in °K and proton speed in km/s respectively, 4th and 5th panels are Dst index and vertical component of IMF both measured in nT.

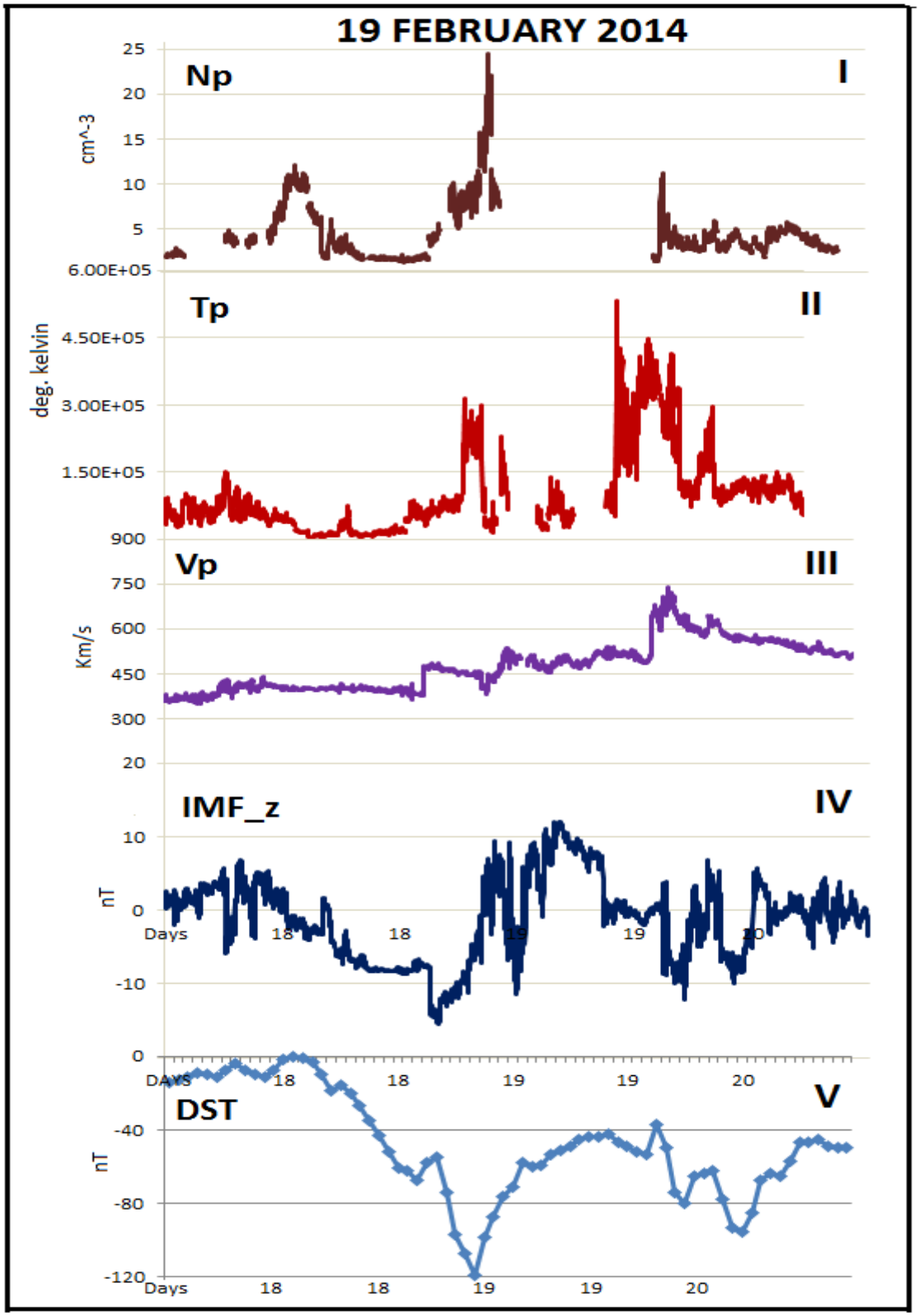

Figure 5: There are five panels in the figure. 1st, 2nd and 3rd panels are solar wind proton density in cm^{-3}, proton temperature in °K and proton speed in km/s respectively, 4th and 5th panels are Dst index and vertical component of IMF both measured in nT.

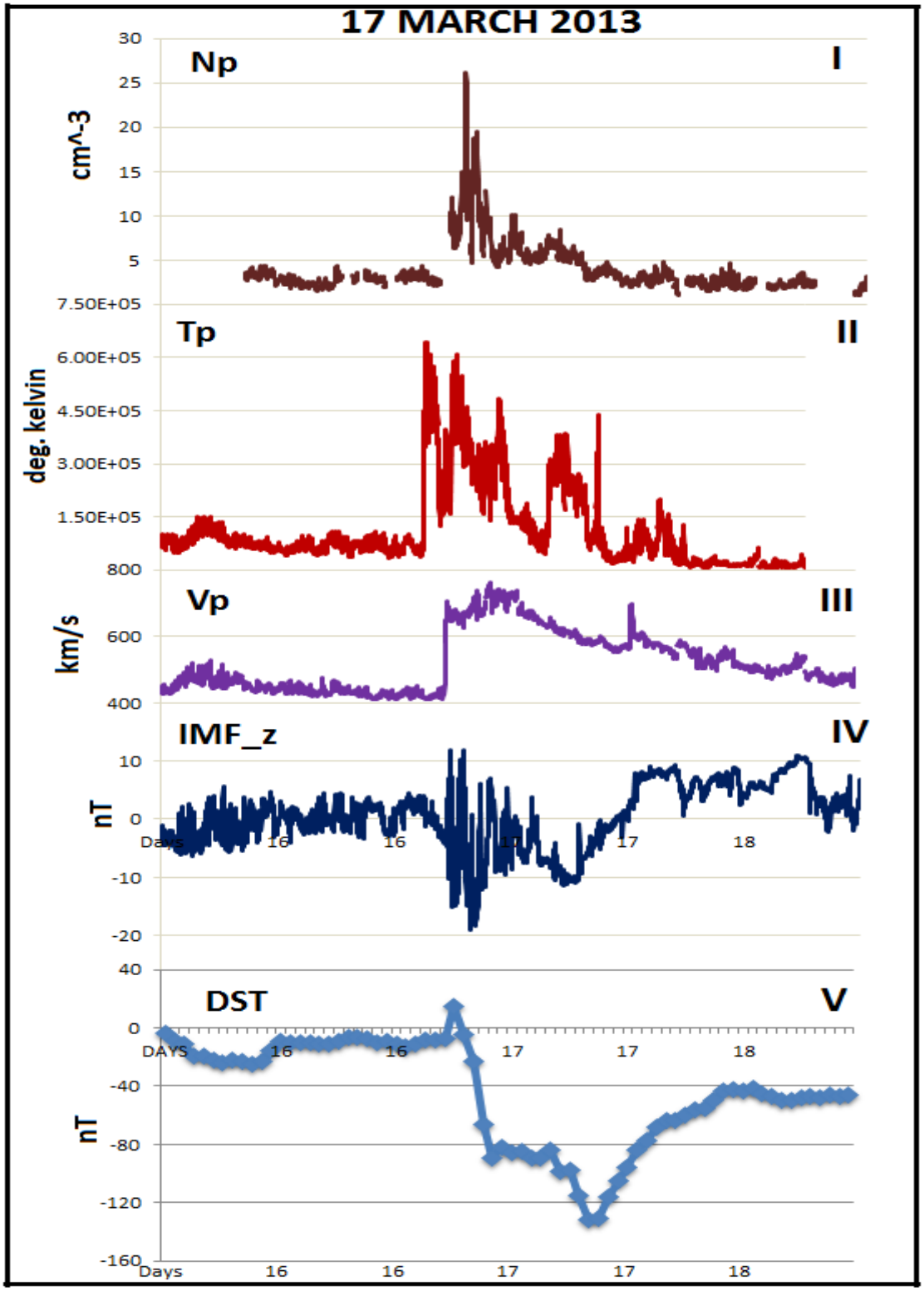

Figure 6: There are five panels in the figure. 1st, 2nd and 3rd panels are solar wind proton density in cm^{-3}, proton temperature in °K and proton speed in km/s respectively, 4th and 5th panels are Dst index and vertical component of IMF both measured in nT.

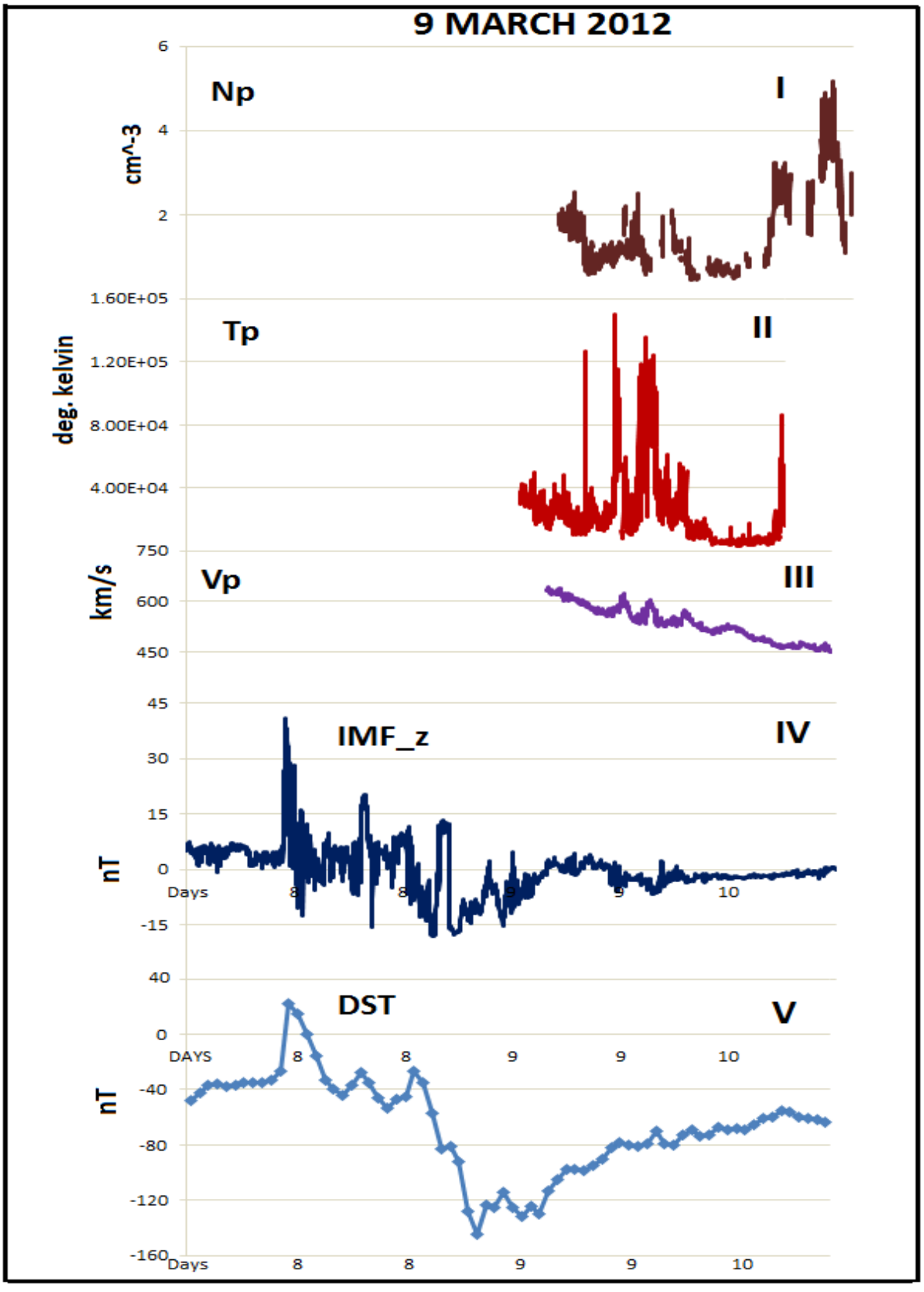

Figure 7: There are five panels in the figure. 1st, 2nd and 3rd panels are solar wind proton density in cm^{-3}, proton temperature in °K and proton speed in km/s respectively, 4th and 5th panels are Dst index and vertical component of IMF both measured in nT.

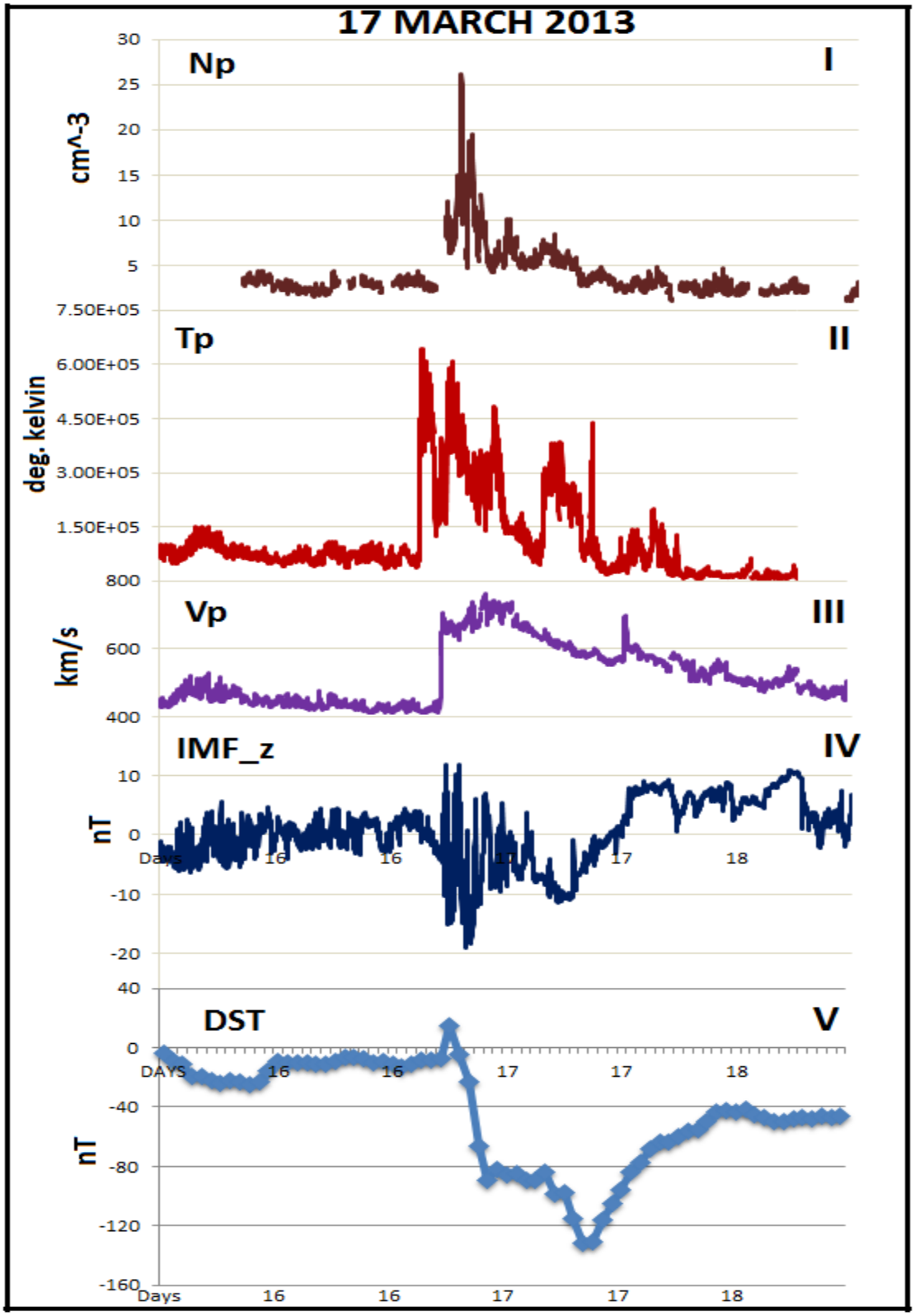

Figure 8: There are five panels in the figure. 1st, 2nd and 3rd panels are solar wind proton density in cm^{-3}, proton temperature in °K and proton speed in km/s respectively, 4th and 5th panels are Dst index and vertical component of IMF both measured in nT.

DISCUSSION

Figure 1, representing event that occur on 23rd June 2015, is the summer strongest event and second strongest event of 24th solar cycle. In this event solar proton density (Np) varying with ~59.43 per cubic centimetre at 18UTC on 22nd June 2015, solar proton temperature (Tp) varying with ~8.47E+05°K at 17UTC on 24th June 2015, solar proton speed (Vp) varying with ~808.31km/s at 6UTC on 23rd June 2015, the vertical component of interplanetary magnetic field (IMF-z) varying with ~ -39.44nT at 18UTC on 22nd June 2015, disturbed storm index (Dst) varying with ~ -204nT at 5UTC on 23rd 2015. The Dst lag IMF-z by 9UTC. For winter geomagnetic storms, the strongest event is on 20th December 2015. In this event the solar proton density (Np) varying with

~38.45cm^{-3} on 20th December 2015 at 12UTC, solar proton Temperature (Tp) varying with ~2.06E+05°K on 19th December 2015 at 16UTC and solar proton speed varying with ~502.04km/s at 20UTC on the same day, vertical component of interplanetary magnetic field (IMF-z) varying with ~ -18.91nT on 20th December 2015 at 22UTC and disturbed storm index (Dst) varying with ~ -155nT at 23UTC on the same day but lag behind IMF-z by 1UTC. In the equinox geomagnetic storm, the strongest event is on 17th March 2015. In this event the solar proton density (Np) varying with ~33.52cm^{-3} on 17th March 2015 at 4UTC and solar proton Temperature (Tp) varying with ~6.17E+05°K at 16UTC on the same day, solar proton speed varying with ~737.924km/s at 21UTC on 18th March 2015, vertical component of interplanetary magnetic field (IMF-z) varying with ~ -28.56nT at 13UTC on 17th March 2015 and disturbed storm index (Dst) varying with ~ -222nT at 23UTC on the same day but lag behind IMF-z with 10UTC.

REFERENCES

[1]Gonzalez, W. D., Tsurutani, B. T., & Clúa de Gonzalez, A. L. (1999). Interplanetary origin of geomagnetic storms. *Space Science Reviews*, *88*(3), 529-562.

[2] Mansilla, G. A. (2014). Solar cycle and seasonal distribution of geomagnetic storms with sudden commencement.

[3] Singh, A. K., Siingh, D., & Singh, R. P. (2010). Space weather: physics, effects and predictability. *Surveys in geophysics*, *31*(6), 581-638.

[4] Tsurutani, B. T., Echer, E., & Gonzalez, W. D. (2011, May). The solar and interplanetary causes of the recent minimum in geomagnetic activity (MGA23): a combination of midlatitude small coronal holes, low IMF B Z variances, low solar wind speeds and low solar magnetic fields. In *Annales Geophysicae* (Vol. 29, No. 5, pp. 839-849). Copernicus GmbH.

[5] Parker, J., & Heywood, D. (1998). The earth and beyond: Developing primary teachers' understanding of basic astronomical events. International Journal of Science Education, 20(5), 503- 520.

[6] Kelly, N. A., & Gibson, T. L. (2009). Improved photovoltaic energy output for cloudy conditions with a solar tracking system. Solar Energy, 83(11), 2092-2102.

[7] A. Rodger and M. Jarvis, "Ionospheric research 50 years ago, today and tomorrow," J. Atmos. Solar-Terrestrial Phys., vol. 62, no. 17–18, pp. 1629–1645, Nov. 2000.

[8] J. R. Woodroffe, S. K. Morley, V. K. Jordanova, M. G. Henderson, M. M. Coweel, and J. G. Gjerloev, (2016) The Latitudinal Variation of Geoelectromagnetic Disturbances During Large (Dstm< -100) Geomagnetic Storm.